Biosensors and Bioelectronics 43 (2013) 257–263

Contents lists available at SciVerse ScienceDirect

Biosensors and Bioelectronics

journal homepage: www.elsevier.com/locate/bios

Sensitive electrochemical analysis of BRAF V600E mutation based on an amplification-refractory mutation system coupled with multienzyme functionalized Fe_3O_4/Au nanoparticles

Bo Situ [a], Nannan Cao [b], Bo Li [a], Qinlan Liu [a], Li Lin [a], Zong Dai [c], Xiaoyong Zou [c], Zhen Cai [a], Qian Wang [a], Xiaohui Yan [d,*], Lei Zheng [a,*]

[a] Department of Laboratory Medicine, Nanfang Hospital, Southern Medical University, Guangzhou 510515, PR China
[b] Department of Laboratory Medicine, Guangdong Provincial Hospital of Traditional Chinese Medicine, Guangzhou 510120, PR China
[c] School of Chemistry and Chemical Engineering, Sun Yat-Sen University, Guangzhou 510275, PR China
[d] Research Center of Clinical Medicine, Nanfang Hospital, Southern Medical University, Guangzhou 510515, PR China

ARTICLE INFO

Article history:
Received 2 November 2012
Received in revised form
2 December 2012
Accepted 6 December 2012
Available online 20 December 2012

Keywords:
Alkaline phosphatase
Amplification-refractory mutation system
BRAF V600E mutation
Cancer
Electrochemical biosensor

ABSTRACT

A novel electrochemical biosensor was developed for the analysis of BRAF V600E mutation in colorectal cancer cell samples based on a dual amplification strategy of amplification-refractory mutation system (ARMS) PCR and multiple enzyme labels. The labeled amplicons were conjugated on Fe_3O_4/Au nanoparticles using Au–S linkages. Alkaline phosphatases were then loaded onto the nanoparticles through biotin–streptavidin interactions. The resultant composite nanoparticles were characterized by transmission electron microscopy, electrochemical impedance spectroscopy, and cyclic voltammetry. In the presence of 2-phospho-L-ascorbic acid, the mutant alleles were quantified on a screen-printed carbon electrode (SPCE) from the anodic current of the enzymatic product, ascorbic acid. BRAF V600E mutant alleles concentrations as low as 0.8% were successfully determined in an excess of wild-type background. In a cell-line dilution model, the proposed method was more sensitive than were DNA sequencing and agarose gel electrophoresis. This work demonstrates a new strategy for sensitivly detecting BRAF V600E variations. It can pave the way for analyzing other rare mutations in complex cancer samples because of its high sensitivity, simplicity, low cost, and easy validation of assay procedures.

1. Introduction

The BRAF mutation, which has been found in diverse human tumors (Moon et al., 2009; Maddodi et al., 2010; Dietrich et al., 2012), has been implicated in causing cancers. An oncogenic mutation (T→A) at nucleotide 1799 accounts for the most frequent of all BRAF genetic abnormalities (Solit et al., 2006). This transversion mutation results in the substitution of valine with glutamate acid in codon 600 (V600E) and converts BRAF into a dominant transforming protein (Mao et al., 2010). Because the response to RAF kinase inhibitors or anti-EGFR therapies depends upon the presence of BRAF V600E variant in cancer cells (Domingo et al., 2005; Di Nicolantonio et al., 2008; Yokota et al., 2011), a reliable diagnostic test for the V600E mutation appears to be greatly desirable.

Detection of V600E mutation from cancer primarily requires analysis of such samples as precancerous or cancerous tissue, ascites, biopsy, stool, and circulating extracellular DNA released in the blood (Milbury et al., 2009). These samples are heterogeneous and often composed of both mutation-containing malignant cells and wild-type benign tissues. In many cases, mutant DNA is present in low abundance among an elevated background of wild-type alleles, making it difficult to discern. Currently, PCR followed by Sanger sequencing is the gold standard in mutation analysis (Tsiatis et al., 2010). Indeed, Sanger sequencing is reliably used to identify hereditary alterations, such as single-nucleotide polymorphism (SNP), because the percentage of these variants is not less than 50% in the genome (Shendure et al., 2004). Nevertheless, a key disadvantage of conventional PCR followed by sequencing in detecting cancerous mutations is the inability to enrich minority DNA variants from tumor cells selectively, resulting in moderate sensitivity (Pinzani et al., 2011). This may lead to false-negative diagnoses in some specimens and therefore has a great effect on decisions of therapy (Mao et al., 2010). Moreover, the expensive and sophisticated sequencing platforms required are

* Corresponding authors. Tel.: +86 20 62787681; fax: +86 20 61642147.
E-mail addresses: gzyanxh@126.com (X. Yan), nfyyzhenglei@smu.edu.cn (L. Zheng).

0956-5663/$ - see front matter © 2012 Elsevier B.V. All rights reserved.
http://dx.doi.org/10.1016/j.bios.2012.12.021

not always affordable for clinical laboratories (James et al., 2006). Thus, there is a pressing requirement for the development of alternative technologies for mutation analysis of cancer samples.

The amplification-refractory mutation system (ARMS) is an effective method to identify mutations involving single nucleotide changes or small deletions (Dempsey et al., 2004). This system is based on the use of sequence-specific PCR primers that allow selective amplification of specific DNA variants only when the target alleles are complementary to the primers (Lacerra et al., 2007). Electrochemical enzyme biosensors are emerging as excellent analytical tools for sensitive and inexpensive genetic detection (Delvaux et al., 2005; Kumar et al., 2007). The sensitivity of an enzyme sensor stems from its extraordinary biocatalysis power, which in turn provides a great amplification of signals (Oaew et al., 2012). Herein, we report a dual amplification strategy for detecting BRAF V600E mutation that combines the advantages of target enrichment by ARMS and signal amplification by enzymatic catalyzing reaction. Fe_3O_4/Au nanoparticles were utilized as carriers for loading enzymes, owing to their multifarious uses, including use in separations, catalysis and delivery (Radwan and Azzazy, 2009). On the one hand, mutant alleles could be amplified by ARMS PCR with high specificity. On the other hand, the incorporation of enzymes (alkaline phosphatases) to generate the output electrochemical signals offered the potential for signal amplification, further improving the sensitivity. In a cell-line dilution study, this method was capable of discerning as few as 0.8% BRAF V600E DNA in an excess of wild-type background.

2. Experimental

2.1. Chemicals and reagents

All oligonucleotide primers were supplied by Shanghai Sangon Biological Engineering Technology and Services Co. Ltd. (China). DNA marker, Mg^{2+} plus buffer, dNTPs, and Taq DNA polymerase were purchased from Takara (Japan). Biotinylated dCTP was obtained from PromoKine (Germany). The E.Z.N.A.® tissue DNA kit was obtained from Omega Bio-Tek (USA). The BigDye terminator cycle sequencing kit was obtained from Applied Biosystems (USA). Nanosep® centrifugal devices were purchased from Pall Corporation (USA). The Fe_3O_4/Au magnetic nanoparticles (100 nm, 5 mg ml^{-1}) in an aqueous suspension were purchased from GoldMag Nanobiotech Co. Ltd. (China). Bovine serum albumin (BSA), streptavidin–alkaline phosphatase (Sa–ALP) and 2-phospho-L-ascorbic acid (AAP) were obtained from Sigma-Aldrich (USA). Agarose was obtained from Biowest (Spain). Aqueous solutions were prepared in ultrapure water (18.2 MΩ cm, Millipore MilliQ water purification system). All other reagents were of analytical grade and were used as received.

2.2. Apparatus

Polymerase chain reactions were performed on a Mastercycler® thermal cycler (Eppendorf, Germany). All agarose gel electrophoresis results were visualized and photographed by UV transillumination using a Gel Doc™ 2000 system (Bio-Rad, USA). Sequencing analysis was run on an ABI3730xl automated capillary sequencer (Applied Biosystems, USA). Disposable screen-printed carbon electrodes (SPCEs) were purchased from DropSens (Spain). The electrode incorporates a conventional three-electrode configuration, which comprises a carbon working electrode (4-mm diameter), a carbon counter electrode, and a silver reference electrode. A sensor connector (DropSens, Spain) enables the SPCE to be connected to an electrochemical workstation. Electrochemical experiments, including cyclic voltammetry (CV), differential pulse voltammetry (DPV) and electrochemical impedance spectroscopy (EIS), were carried out on a CH660C electrochemical workstation (Shanghai CH Instrument, China) connected to a personal computer. Transmission electron microscope (TEM) images were obtained on a H-7650 transmission scanning electron microanalyzer (Hitachi Instruments, Japan) equipped with a CCD camera.

2.3. Cell lines and genomic DNA

Human colon adenocarcinoma cell lines were kindly provided by the Institute of Gastroenterology, Nanfang Hospital, Guangzhou, China. The cell line HT29 harbors a heterozygous BRAF V600E mutation while the SW480 harbors a BRAF wild-type. Genomic DNA (gDNA) was extracted and purified from cultured cells with the E.Z.N.A.® tissue DNA kit according to the instruction. The concentration of the extracted DNA was measured by a spectrophotometer at 260 nm.

2.4. ARMS amplification

Special forward and reverse primers were designed and optimized to amplify the BRAF V600E alleles selectively (Table S1). The reaction was carried out in a final volume of 20 μl and contained the following: 10 × PCR Mg^{2+} plus buffer; a dNTP mixture of 50 μM dCTP, 50 μM biotin–dCTP, 100 μM each of dATP, dTTP, and dGTP; 0.5 U of Taq DNA polymerase; 250 nM of each forward and reverse primer; and 30 ng of DNA template. The PCR cycle comprised an initial activating step at 95 °C for 30 s, a cycling step (45 cycles) performed as follows: 95 °C for 10 s, 67 °C for 25 s, and 72 °C for 30 s, and a final extension at 72 °C for 3 min.

2.5. Enzyme-linked electrochemical detection of ARMS amplicons

ARMS amplification products were initially cleaned up using Nanosep® centrifugal devices, and then added to 50 μl of 5 mg ml^{-1} Fe_3O_4/Au nanoparticles (in 0.1 M Tris–HCl, pH 7.4) solution and shaken slightly for 6 h at 4 °C. Thereafter, the DNA–nanoparticle complex suspension was incubated with 500 μl of 5% BSA for 30 min at room temperature to block the non-specific binding sites. After magnetic separation, the composite nanoparticles were rinsed with distilled water to remove unbound BSA, and then added to 50 μl of 0.02 mg ml^{-1} Sa-ALP for 15 min to incubate at room temperature to form the biotin–streptavidin linkages. Unbound components were removed by washing the nanoparticles twice in a magnetic field with 500 μl Tris–HCl (0.1 M, pH 7.4). The nanoparticles were then re-dispersed in 50 μl of 75 mM AAP (in 0.1 M Tris–HCl, pH 9.0, 1 mM $MgCl_2$) solution and incubated for 40 min at 37 °C with shaking. The enzymatic reaction was stopped by the addition of 2 μl of 0.1 M disodium EDTA. After magnetic separation, 5 μl of the resulting solution was mixed with 45 μl of sodium acetate buffer (0.1 M, pH 5.5). The reaction mixture (50 μl) was then dropped onto the SPCE reservoir area to cover the working, counter, and reference electrodes. The electrochemical behavior of the reaction products was examined by CV and DPV. Analyses were always made in triplicate.

2.6. DNA sequencing and agarose gel electrophoresis analysis

For sequence analysis, genomic DNA isolated from the cancer cells as described in Section 2.3 was initially amplified by conventional PCR. Amplification of the BRAF gene, exon 15 was performed in 20 μl reaction volume containing 10 × PCR Mg^{2+} plus buffer, a dNTP mixture of 100 μM each of dCTP, dATP, dTTP,

and dGTP, 0.5 U of Taq DNA polymerase, 250 nM of each forward and reverse primer (Table S1), and 30 ng of DNA template. The conventional PCR amplification protocol comprised an initial activating step at 95 °C for 30 s, a cycling step (40 cycles) performed as follows: 95 °C for 10 s, 54 °C for 20 s and 72 °C for 30 s, and a final extension at 72 °C for 3 min. The PCR products were purified and sequenced directly from both sides with the same primers using the BigDye terminator cycle sequencing kit on an ABI3730xl automated capillary sequencer.

For comparison, the products were also detected by gel electrophoresis. The ARMS reactions were carried out under the same condition without adding biotin–dCTP. A volume of 5 μl of the ARMS amplicons was resolved by 2% (w/v) agarose gel containing ethidium bromide and then electrophoresed at 100 V for 30 min. The results were visualized and photographd by UV transillumination.

3. Results and discussion

3.1. Principle of the sensing assay

The basic principle of this method is outlined in Fig. 1. Initially, a novel method was developed that incorporates thiol groups and multiple biotin labels within an ARMS reaction to amplified V600E target alleles. ARMS is an effective amplification approach to enrich the proportion of mutant alleles and relies on the utilization of 3′ terminal nucleotide manipulation to a particular nucleotide variant. The success of allelic discrimination depends on the inability of DNA polymerase to extend mismatch primers during PCR (Clayton et al., 2000). As shown in step A, the thiolated primer was included during the ARMS reaction as part of the duplex. Meanwhile, the products were tagged with biotin molecules by the incorporation of biotinylated dCTP in the reaction. Step B illustrates the fabrication process of the multienzyme functionalized Fe_3O_4/Au nanoparticles. The thiolated amplicons were captured onto the Fe_3O_4/Au nanoparticles through the strong affinity of thiols to gold surfaces. Bovine serum albumin was then added to block the non-specific binding sites by Au–protein interactions. After incubation with composite nanoparticles, Sa–ALPs were linked to the DNA through biotin–streptavidin conjugation. Hence, the amount of ALP that loaded on the nanoparticles was related to the quantity of amplicons. Since ascorbic acid was the product of the enzymatic hydrolysis reaction, the detection of mutant alleles could then be realized by measuring the oxidation current of ascorbic acid (AA) on an SPCE (Step C). This strategy enables mutation analysis by converting the identification of specific DNA variations to the electrochemical measurements of enzymatic reaction, thus amplifying the detection response.

3.2. Incorporation of biotin–dCTP in ARMS amplification

A forward primer with the last base that matches the V600E mutation but mismatches the wild-type nucleotide was designed

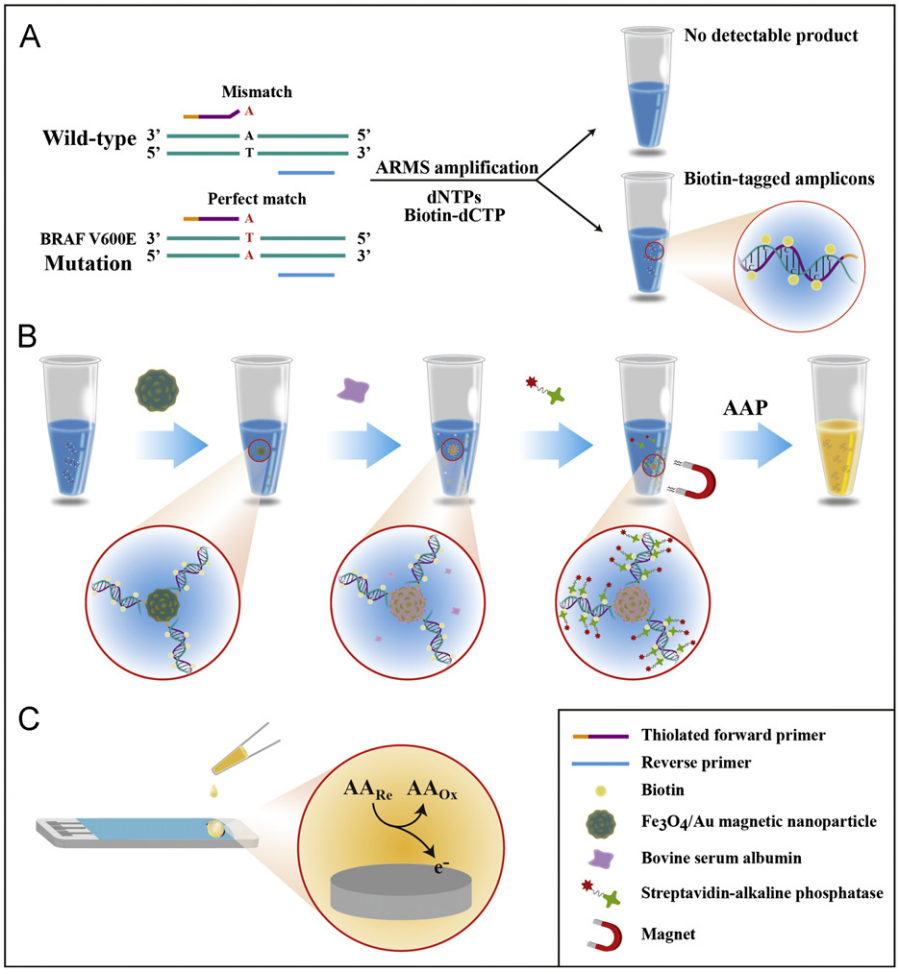

Fig. 1. Representative diagram for the electrochemical sensing assay of BRAF V600E mutation. (A) ARMS amplification with thiol groups and biotin labels. (B) The fabrication process of the multienzyme functionalized Fe_3O_4/Au nanoparticles. (C) Oxidation of ascorbic acid at an SPCE.

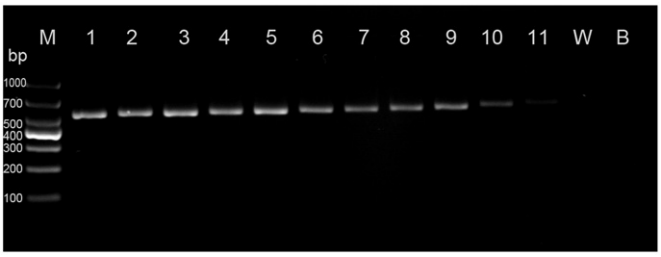

Fig. 2. Optimization study on biotinylated dCTP incorporation in ARMS. The percentage of biotin–dCTP (lanes 1–11) titrated was between 0% and 100%. Lane M, DNA marker; lanes W and B, amplified products from negative control (genomic DNA of wild-type SW480 cell line) and blank (distilled water), respectively. Amplicons were electrophoresed on 2% agarose gel.

and optimized. As illustrated in the electropherogram (Fig. 2), under the optimized conditions, wild-type and V600E variation at nucleotide 1799 of BRAF oncogene were clearly discriminated. The products amplified from mutant BRAF V600E gDNA revealed corresponding bands in the gel, whereas those from the wild-type did not present any bands, indicating the selective amplification with high specificity by ARMS.

Furthermore, by adding biotin-modified dCTP into PCR reaction, ARMS amplicons were successfully labeled with biotin molecules in the reactions. To evaluate the incorporation of biotin–dCTP in the PCR reaction, a total concentration of biotinylated and natural dCTP was maintained at 100 μM. The biotin–dCTP was titrated between 0% and 100%. The PCR products were run on electrophoresis in a 2% agarose gel. As shown in Fig. 2, with an increase in percentage of biotinylated dCTP, a corresponding decrease in the mobility of the products was observed. This change may be due to the large bulk introduced by the biotin molecules (Lo et al., 1988). While high incorporations were achievable, amplification yield was compromised. The decrease of the amplicons showed that Taq DNA polymerase incorporated natural dCTP with greater efficiency than biotinylated dCTP. For high labeling rates without a significant reduction in yield, a 50% of biotin–dCTP was chosen in the follow-up ARMS experiments. Compared with routine DNA labeling approaches that use 5′-terminal functionalized primers (such as primers chemically modified with biotin or digoxin), a major benefit of the proposed method was uniform distribution of modifications across each DNA duplex. Thus, each replica was capable of binding a large amount of enzymes by streptavidin–biotin interactions, resulting in a multienzyme labeling assay as part of a signal amplification strategy.

3.3. Characterization of the composite nanoparticles

Recently, hybrid nanomaterials have attracted much attention owing to their novel combined properties and potential applications. Fe_3O_4/Au nanoparticles consist of an inner iron oxide core and an outer shell of gold nanoparticle seeds; this combination not only provides a magnetic property for ready separation from reaction mixtures via an external magnet, but also helps to conjugate various biomolecules through binding of gold to sulfur-, phosphor-, or nitrogen-based ligands or non-covalent interactions (Zhang et al., 2011; Chuah et al., 2012). In this work, Fe_3O_4/Au nanoparticles were utilized as vehicles to load alkaline phosphatase by conjugates of multienzyme functionalized sequences.

The morphology of the composite nanoparticles was characterized by TEM. As shown in Figs. 3A and S1, the nanoparticles were dispersible and stable in Tris–HCl buffer at pH 7.4. The average diameter of the Fe_3O_4/Au particles was about 100 nm. After incubation with PCR amplicons, BSA and Sa–ALP, the nanoparticles were blurred by a layer of electron-lucent substance (Fig. 3B). This confirmed that the proteins were attached to the surface of the Fe_3O_4/Au nanoparticles.

Electrochemical impedance spectroscopy is a powerful tool for investigating the interface features on conductive surfaces. To characterize the changes of the composite nanoparticles, bare Fe_3O_4/Au, DNA/Fe_3O_4/Au, BSA/DNA/Fe_3O_4/Au, and ALP/BSA/DNA/Fe_3O_4/Au nanoparticles were immobilized on the SPCEs by magnetic adsorption. The EIS of different nanoparticles complexes in equivalent $Fe(CN)_6^{3-/4-}$ solution is shown in Fig. 3C. A semicircle of about 100 Ω diameter with an almost straight tail line was obtained at the bare SPCE (Fig. 3C, curve a). The semicircle was increased to 350 Ω diameter at the Fe_3O_4/Au (Fig. 3C, curve b). However, the diameter of the high frequency semicircle was apparently increased to 700 Ω at the DNA/Fe_3O_4/Au complexes (Fig. 3C, curve c), demonstrating a decelerated effect due to the electrostatic repulsion between ferri/ferrocyanide and the phosphate groups contained on DNA (Hassen et al., 2008). Moreover, the diameters of the semicircles were increased to 910 Ω (BSA/DNA/Fe_3O_4/Au) and 1200 Ω (ALP/BSA/DNA/Fe_3O_4/Au) (Fig. 3C, curves d and e), indicating a further increase of the charge transfer resistance. The results may be attributed to the low conductivity of Fe_3O_4/Au nanoparticles surrounded by enzyme-bearing DNA sequences.

The electrochemical features of the composite nanoparticles were also investigated by CV. As shown in Fig. 3D, curve a, a pair of quasi-reversible redox peaks of $Fe(CN)_6^{3-/4-}$ with a peak separation (ΔE_p) of 278 mV was obtained for the bare SPCE. The peak currents reduced with an increased ΔE_p of 369 mV at Fe_3O_4/Au (Fig. 3D, curve b). For the DNA/Fe_3O_4/Au nanoparticles, the peak currents attenuated further with an increased ΔE_p of 430 mV (Fig. 3D, curve c), indicating that the binding DNA made the interface electron transfer harder. Furthermore, significant enhancement of the ΔE_p to 608 mV and 646 mV with decreased peak currents were observed for BSA/DNA/Fe_3O_4/Au (Fig. 3D, curve d) and ALP/BSA/DNA/Fe_3O_4/Au (Fig. 3D, curve e), respectively, which can be ascribed to the further reduced electron transfer kinetics at the protein-coated nanoparticles. These results were consistent with EIS data, indicating the successful conjugation of DNA and proteins on the Fe_3O_4/Au nanoparticles.

3.4. Electroanalysis of products and substrates of ALP

Alkaline phosphatase (ALP) catalyzes the hydrolysis of phosphate esters in an alkaline environment, resulting in the formation of an organic radical and inorganic phosphate (Wilson and Rauh, 2004). In electrochemical sensing assays, ALP is commonly used to generate electroactive products, most of which can be detected and quantified. In this study, AAP was selected as the ALP substrate for its low cost, good stability, non-fouling, commercial availability, and sensitive amperometric response (Preechaworapun et al., 2008). Ascorbic acid is the product of the ALP enzymatic hydrolysis reaction of AAP, as shown in reaction (1). Ascorbic acid can then be detected via direct oxidation on the electrode, as shown in reaction (2) (Kokado et al., 2000). The individual electrochemical behavior of AA and AAP was examined by CV. As shown in Fig. S2, AA and AAP could be well defined without interference at SPCEs.

Enzyme reaction:

$$\text{2-phospho-L-ascorbic acid} + H_2O \xrightarrow[\text{alkaline condition}]{\text{ALP}} \text{ascorbic acid} + H_3PO_4 \quad (1)$$

Electrochemical reaction:

$$\text{ascorbic acid} \rightarrow \text{dehydroascorbic acid} + 2H^+ + 2e^- \quad (2)$$

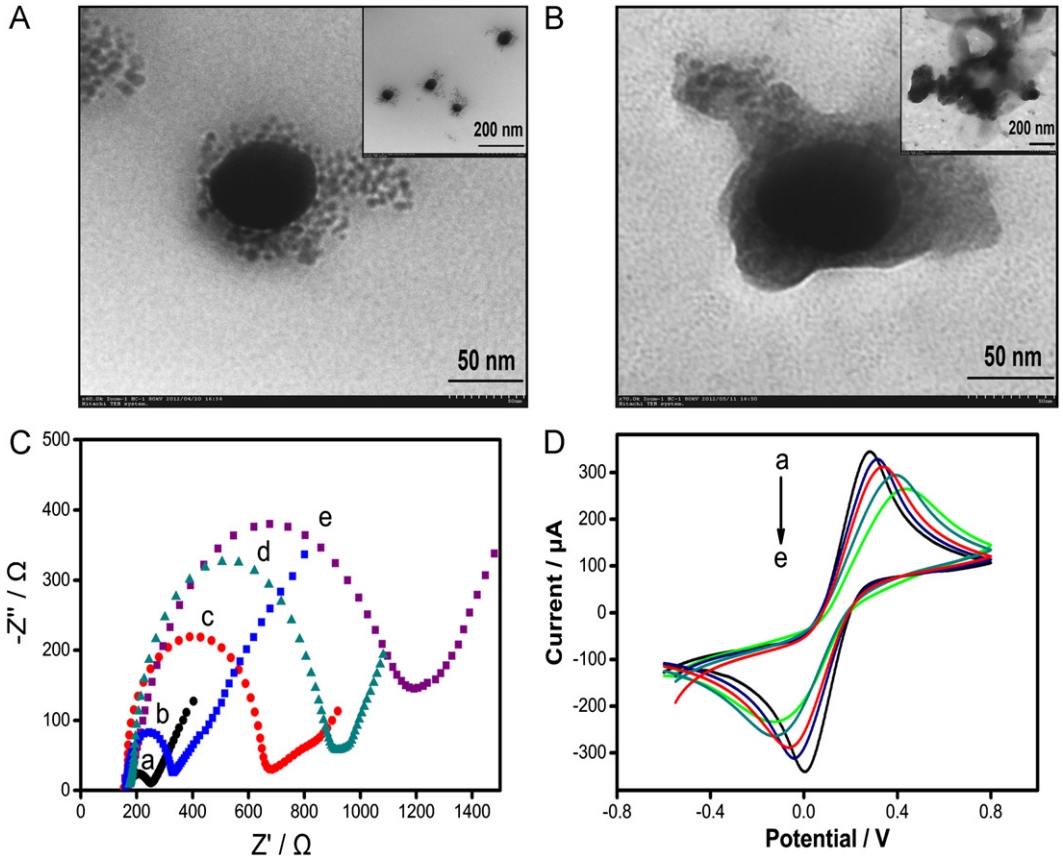

Fig. 3. TEM images of (A) Fe_3O_4/Au nanoparticles and (B) ALP/BSA/DNA/Fe_3O_4/Au composite nanoparticles. (C) Complex plane impedance plots in 10 mM $K_3[Fe(CN)_6]$: $K_4[Fe(CN)_6]$ (1:1) mixture containing 0.1 M KCl of bare SPCE (a); Fe_3O_4/Au (b); DNA/Fe_3O_4/Au (c); BSA/DNA/Fe_3O_4/Au (d); and ALP/BSA/DNA/Fe_3O_4/Au (e) at SPCEs. (D) Cyclic voltammograms of bare SPCE (a); Fe_3O_4/Au (b); DNA/Fe_3O_4/Au (c); BSA/DNA/Fe_3O_4/Au (d); and ALP/BSA/DNA/Fe_3O_4/Au (e) in 10 mM $Fe(CN)_6^{3-/4-}$ in 0.1 M KCl solution at SPCEs. Scan rate: 100 mV s^{-1}.

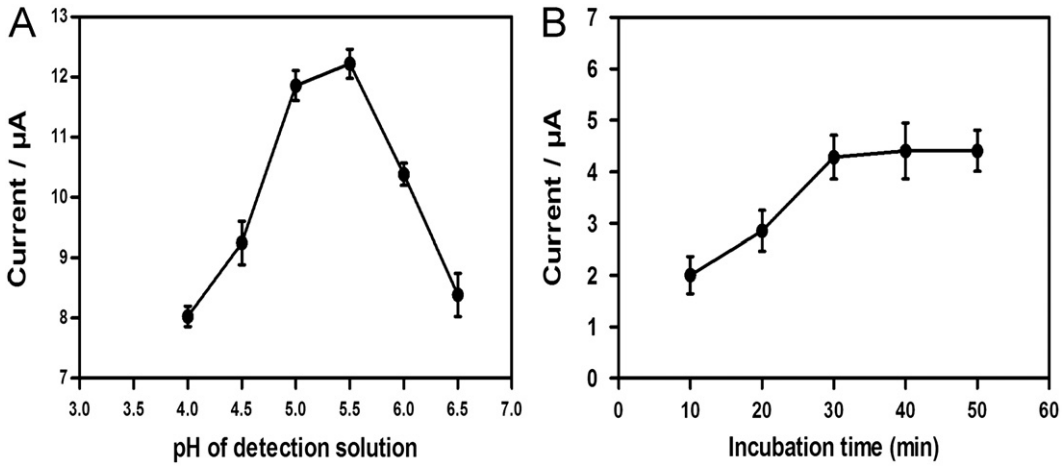

Fig. 4. Optimization of experimental conditions. (A) Effect of pH value (from 4.0 to 6.5) in the presence of 1 mM ascorbic acid. (B) Plot of peak current response versus incubation time. The enzymatic reaction products were analyzed in 0.1 M sodium acetate buffer solution (pH 5.5).

The effect of solution pH on the electrochemical responses of AA was investigated by DPV. As shown in Fig. 4A, the peak current of AA was greatly influenced by pH. When the pH was below 5.5, the oxidation peak current increased along with the increasing pH. When the pH was larger than 5.5, the peak current was greatly attenuated. The maximal anodic peak current was obtained at pH 5.5, which was adopted as the optimum pH value for AA detection. The incubation time of the enzymatic reaction was also studied. Fig. 4B shows the effects of incubation time from 10 to 50 min on the signal responses of the enzymatic hydrolysis products. One can observe that the peak current enhanced gradually with the augment of incubation time and then tended to be constant after about 30 min, which indicated that equilibrium was reached. To obtain the maximum hydrolysis efficiencies, 40 min was selected for the enzymatic reaction.

3.5. *Analysis of cancer cell samples*

To evaluate the performance of the proposed method for analysis of mutation in tumor cells, serial dilutions of

V600E-mutated (HT29) and wild-type (SW480) DNA were prepared to obtain reconstituted samples containing 50%, 25%, 12.5%, 6.2%, 3.1%, 1.6%, 0.8%, 0.4%, and 0% of mutant alleles. These samples were submitted to ARMS amplification, followed by enzyme-linked electrochemical analysis under the optimum conditions. Fig. 5A shows the DPV response curves for the relationship between the peak current and the percentage of mutant alleles. As shown, AAP and the enzymatic reaction product, AA, show oxidation peaks with the peak potential at 750 mV and 280 mV, respectively. It was clear that the peak current of AAP attenuated with the increase of the percentage of V600E alleles. On the contrary, the anodic peak current of AA was gradually enhanced with incremental concentration of mutant DNA. These phenomena might be attributed to the increase in the amount of enzymes loaded on the nanoparticles with the rise in mutant template. The increase in anodic current of AA was proportional to the percentage of V600E-mutant alleles in the range of 50–0.8%; the linear regression equation was I_p (μA)=3.59+0.53c_{V600E} (%) with a correlation coefficient of 0.977. Peak currents of AA from different percentages of V600E alleles at SPCEs are shown in Fig. 5B. A threshold value was calculated from the mean plus three standard deviations of the negative control. The results demonstrate that the amperometric signals were greater than the threshold value for all dilutions of mutant alleles from 50% to 0.8%, but were below the threshold value for 0.4% and wild-type samples. These data indicate that the present method is capable of identifying BRAF V600E mutation in cancer cells

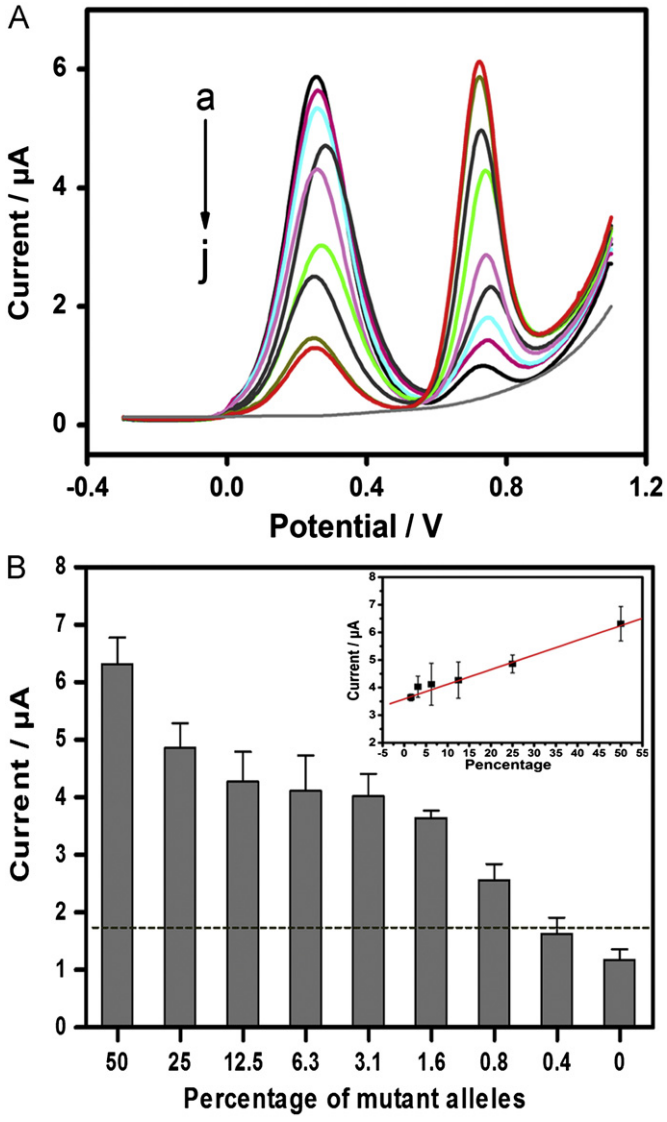

Fig. 5. (A) Differential pulse voltammetry response curves of the assay at various mutant DNA concentrations, from 50% to 0%, and the background response (a–j). DPV conditions: amplitude, 0.05 V; pulse width, 0.05 s; pulse period, 0.5 s. (B) Peak currents of ascorbic acid (AA) from different percentages of V600E alleles at SPCEs. Values are the mean of three replicates and error bars represent the standard deviation (SD). The dashed line represents the threshold value for BRAF V600E mutation. Inset: plot of oxidation peak current versus concentration of the mutant alleles.

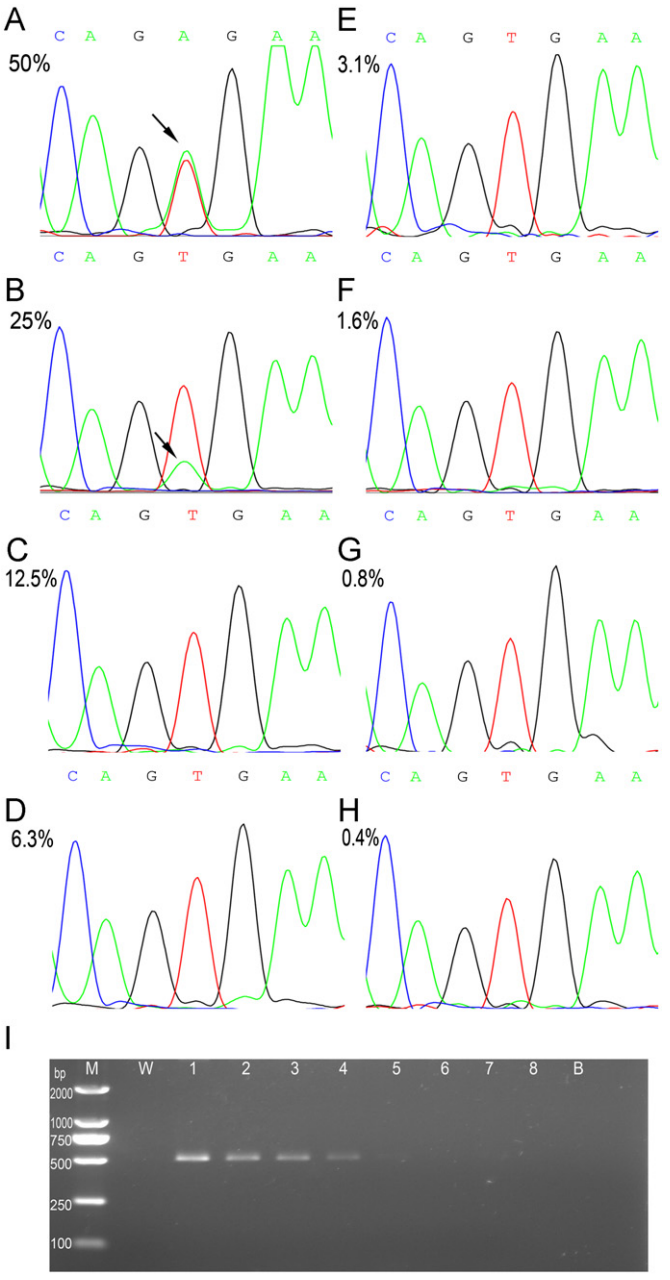

Fig. 6. DNA sequencing and agarose gel electrophoresis for the analysis of cell DNA dilutions samples. (A–H) chromatograms of sequencing analysis from serial dilutions at known percentages (50%, 25%, 12.5%, 6.3%, 3.1%, 1.6%, 0.8%, and 0.4%) harbor V600E alleles. Arrows indicate the appearance of mutant nucleotides. (I) Electropherogram of ARMS products from the same dilutions samples. Lanes 1–8 represent amplicons from serial dilutions at mutant percentages of 50%, 25%, 12.5%, 6.3%, 3.1%, 1.6%, 0.8%, and 0.4%, respectively; lanes W and B, amplified products from negative control (genomic DNA of wild-type SW480 cell line) and blank (distilled water); lane M, DNA marker. Amplicons were electrophoresed on 2% agarose gel.

samples with high specificity. Under optimum conditions, it was possible to discern as little as 0.8% of V600E from cancer cells in a wild-type background.

To assess the performance of our assay against DNA sequencing and agarose gel electrophoresis, we compared the results obtained from the analysis of the same reconstituted samples, as depicted in Fig. 6. By direct sequencing, 25% or more of cell-line DNA known to harbor V600E could be identified with confidence by the presence of an additional mutant peak (Fig. 6, A and B). At lower concentrations, the mutant peak was no longer detectable (Fig. 6, C–H), indicating that the sensitivity of the sequencing was 25%. Agarose gel electrophoresis was also performed with the cell-line samples. An electropherogram of the sensitivity study demonstrated that only dilutions of 6.2% and above presented expected bands; in other words, the limit of detection of agarose gel electrophoresis was 6.2% (Fig. 6I). Our results show that the sensitivity of the described method is much higher than those of Sanger sequencing (25%) and agarose gel electrophoresis (6.2%), and is comparable to those of very sensitive assays, such as pyrosequencing (2%; Tan et al., 2008) or real-time PCR (2%; Jarry et al., 2004).

4. Conclusions

In summary, a novel enzyme-linked electrochemical sensing assay for the analysis of BRAF V600E variations in colorectal cancer cells was established and evaluated. In combination with target amplification by ARMS with signal enhancement by multi-enzyme functionalized Fe_3O_4/Au nanoparticles, it was capable of revealing mutations present in extremely low abundance within an elevated background of wild-type sequences. We demonstrated that this method was more sensitive than DNA sequencing and agarose gel electrophoresis in a cell-line dilution model. The present method is simple, specific, and cost-effective and it does not require sophisticated instrumentations or biohazardous reagents. Moreover, the advantage of the developed method to detect even 0.8% of BRAF V600E may be of importance when only samples with a low proportion of cancer cells are available. It represents a compelling alternative to established molecular diagnostics techniques and opens a versatile way for discerning other hotspot mutations in clinical specimens.

Acknowledgments

This work was supported by the National Natural Science Foundation of China (81271932), the Natural Science Foundation of Guangdong Province (S2011010003840), and the Science and Technology Planning Project of Guangdong Province (2010A030300006, 2012B050600021). We are grateful to Dr. Zhang for kind assistance with TEM imaging.

Appendix A. Supporting information

Supplementary data associated with this article can be found in the online version at http://dx.doi.org/10.1016/j.bios.2012.12.021.

References

Chuah, K., Lai, L.M., Goon, I.Y., Parker, S.G., Amal, R., Justin Gooding, J., 2012. Chemical Communications 48, 3503–3505.
Clayton, S.J., Scott, F.M., Walker, J., Callaghan, K., Haque, K., Liloglou, T., Xinarianos, G., Shawcross, S., Ceuppens, P., Field, J.K., Fox, J.C., 2000. Clinical Chemistry 46, 1929–1938.
Delvaux, M., Walcarius, A., Demoustier-Champagne, S., 2005. Biosensors and Bioelectronics 20, 1587–1594.
Dempsey, E., Barton, D.E., Ryan, F., 2004. Clinical Chemistry 50, 773–775.
Di Nicolantonio, F., Martini, M., Molinari, F., Sartore-Bianchi, A., Arena, S., Saletti, P., De Dosso, S., Mazzucchelli, L., Frattini, M., Siena, S., Bardelli, A., 2008. Journal of Clinical Oncology 26, 5705–5712.
Dietrich, S., Glimm, H., Andrulis, M., von Kalle, C., Ho, A.D., Zenz, T., 2012. The New England Journal of Medicine 366, 2038–2040.
Domingo, E., Niessen, R.C., Oliveira, C., Alhopuro, P., Moutinho, C., Espin, E., Armengol, M., Sijmons, R.H., Kleibeuker, J.H., Seruca, R., Aaltonen, L.A., Imai, K., Yamamoto, H., Schwartz Jr., S., Hofstra, R.M., 2005. Oncogene 24, 3995–3998.
Hassen, W.M., Chaix, C., Abdelghani, A., Bessueille, F., Leonard, D., Jaffrezic-Renault, N., 2008. Sensors and Actuators B: Chemical 134, 755–760.
James, M.R., Dumeni, T., Stark, M.S., Duffy, D.L., Montgomery, G.W., Martin, N.G., Hayward, N.K., 2006. Clinical Chemistry 52, 1675–1678.
Jarry, A., Masson, D., Cassagnau, E., Parois, S., Laboisse, C., Denis, M.G., 2004. Molecular and Cellular Probes 18, 349–352.
Kokado, A., Arakawa, H., Maeda, M., 2000. Analytica Chimica Acta 407, 119–125.
Kumar, A., Aravamudhan, S., Gordic, M., Bhansali, S., Mohapatra, S.S., 2007. Biosensors and Bioelectronics 22, 2138–2144.
Lacerra, G., Musollino, G., Di Noce, F., Prezioso, R., Carestia, C., 2007. Haematologica 92, 254–255.
Lo, Y.M., Mehal, W.Z., Fleming, K.A., 1988. Nucleic Acids Research 16, 8719.
Maddodi, N., Bhat, K.M., Devi, S., Zhang, S.C., Setaluri, V., 2010. Journal of Biological Chemistry 285, 242–254.
Mao, C., Liao, R.Y., Chen, Q., 2010. Journal of Cancer Research and Clinical Oncology 136, 1293–1294.
Milbury, C.A., Li, J., Makrigiorgos, G.M., 2009. Clinical Chemistry 55, 632–640.
Moon, H.J., Kwak, J.Y., Kim, E.K., Choi, J.R., Hong, S.W., Kim, M.J., Son, E.J., 2009. Annals of Surgical Oncology 16, 3125–3131.
Oaew, S., Charlermroj, R., Pattarakankul, T., Karoonuthaisiri, N., 2012. Biosensors and Bioelectronics 34, 238–243.
Pinzani, P., Santucci, C., Mancini, I., Simi, L., Salvianti, F., Pratesi, N., Massi, D., De Giorgi, V., Pazzagli, M., Orlando, C., 2011. Clinica Chimica Acta 412, 901–905.
Preechaworapun, A., Dai, Z., Xiang, Y., Chailapakul, O., Wang, J., 2008. Talanta 76, 424–431.
Radwan, S.H., Azzazy, H.M., 2009. Expert Review of Molecular Diagnostics 9, 511–524.
Shendure, J., Mitra, R.D., Varma, C., Church, G.M., 2004. Nature Reviews Genetics 5, 335–344.
Solit, D.B., Garraway, L.A., Pratilas, C.A., Sawai, A., Getz, G., Basso, A., Ye, Q., Lobo, J.M., She, Y., Osman, I., Golub, T.R., Sebolt-Leopold, J., Sellers, W.R., Rosen, N., 2006. Nature 439, 358–362.
Tan, Y.H., Liu, Y., Eu, K.W., Ang, P.W., Li, W.Q., Salto-Tellez, M., Iacopetta, B., Soong, R., 2008. Pathology 40, 295–298.
Tsiatis, A.C., Norris-Kirby, A., Rich, R.G., Hafez, M.J., Gocke, C.D., Eshleman, J.R., Murphy, K.M., 2010. The Journal of Molecular Diagnostics 12, 425–432.
Wilson, M.S., Rauh, R.D., 2004. Biosensors and Bioelectronics 20, 276–283.
Yokota, T., Ura, T., Shibata, N., Takahari, D., Shitara, K., Nomura, M., Kondo, C., Mizota, A., Utsunomiya, S., Muro, K., Yatabe, Y., 2011. British Journal of Cancer 104, 856–862.
Zhang, B., Tang, D., Liu, B., Chen, H., Cui, Y., Chen, G., 2011. Biosensors and Bioelectronics 28, 174–180.